

The Influence of Percolation in the generalized Chalker–Coddington Model

Marcus METZLER

Department of Physics, Toho University, Miyama 2-2-1, Funabashi, Chiba 274-8510

(Received)

We numerically investigate the influence of classical percolation on the quantum Hall localization-delocalization transition. This is accomplished within the framework of the generalized Chalker–Coddington network model which allows us to control the number of *classical* saddle points by setting the width W of the saddle point distribution. It is found that increasing this width causes a new microscopic length scale to appear which depends on W and scales with the exponent $X \approx 1.36$ which indicates a close connection to the classical percolation length ξ and its exponent $\nu_p = 4/3$. Furthermore, the influence of an increase in W on the spectral statistics of the quasienergies of the network model is investigated. An effect similar to the increase of the potential correlation length in the Landau model is seen.

KEYWORDS: Chalker–Coddington model, level spacing distribution, scaling, quantum Hall systems, multifractality

§1. Introduction

The Chalker–Coddington network¹⁾ is a model for quantum Hall systems with long ranged disorder potentials. It represents a system of two-dimensional (2D) electrons in a strong magnetic field and smooth disorder potential. As a member of the quantum Hall universality class²⁾ it has been used to determine various critical quantities at the localization-delocalization (LD) transition point between the quantized plateaus of the Hall conductance.^{1, 3, 4, 5)}

The model is based on the semi-classical time evolution picture of 2D electrons moving along the equipotential contours of a smooth disorder potential under the influence of a strong magnetic field. The electronic states are defined by the amplitudes on the network links representing the equipotential contours and the time evolution is determined by unitary scattering matrices at the nodes of the network corresponding to the saddle points of the random potential where tunneling between contours occurs. The scattering strength is determined by the electron energy and the energy of the saddle point. In contrast to the original network model introduced by Chalker and Coddington, who explicitly excluded any percolation effects by setting all saddle point energies to zero, the generalized version of the model allows percolation effects by introducing an energy range $[-W, W]$ for the distribution of saddle point energies.^{3, 4, 5)} While this generalization of the model does not change the critical behavior as long as the investigated systems are large enough, it introduces a microscopic length scale a that depends on W/E_t , where E_t is the tunneling energy at the saddle points.⁵⁾ Since the motion of electrons with energy E at saddle points with energies u_k that obey $|u_k - E| \gg E_t$ follows the classical path, it was concluded in refs. 5 and 7 that this length scale must be connected to the classical percolation length, meaning that a scales

with the classical percolation exponent $\nu_p = 4/3$, i.e.

$$a \left(\frac{W}{E_t} \right) \propto \left(\frac{W}{E_t} \right)^{\nu_p}. \quad (1)$$

As long as the system size L is much larger than this length scale the generalized model will show the same critical properties as the original.

In the following we will first give a short description of the generalized Chalker–Coddington model followed by a review of the arguments given in refs. 5 and 7 for the influence of percolation effects. We will then give numerical evidence that the microscopic length scale indeed shows the scaling behavior we expected. After that we take a look at the spectral properties of the network model and their dependence on W . We will show that the shape of the level spacing distribution function at criticality changes more and more to Poissonian behavior with increasing W . This is also the case for the number variance and consequently the spectral compressibility. In spite of these changes the scaling exponent ν seems to be unaffected. The change of shape in the level spacing distribution is similar to that observed by Ono et al.²¹⁾ when increasing the correlation length of the disorder potential.

§2. The Network Model

As we have already mentioned the Chalker–Coddington model is based on the semi-classical picture of electrons in two dimensions moving under the influence of a strong perpendicular magnetic field B in a long-ranged disorder potential V , i.e. the correlation length l_V of V is large compared to the magnetic length $l_c = \sqrt{\hbar c/eB}$. Starting from this picture the following network model was developed.^{1, 8)}

The network consists of a 2D regular lattice (see Fig. 1) whose links are unidirectional channels and whose nodes are scattering centers represented by 2×2 unitary scattering matrices S^k , where k is the node index. The ma-

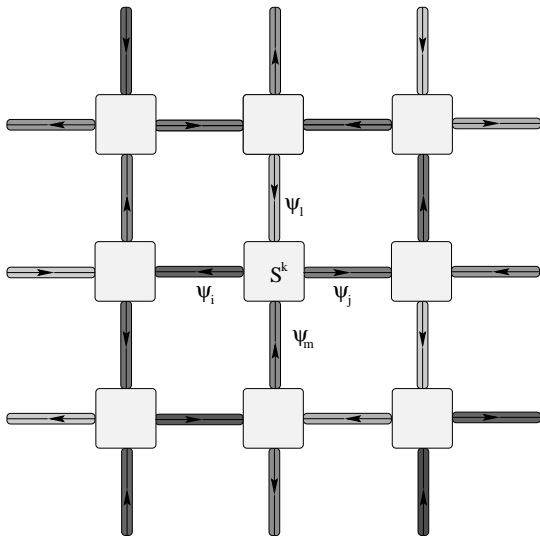


Fig. 1. The Chalker-Coddington network model. At each saddle point the matrix S^k describes the scattering from incoming to outgoing channels. The network operator U performs the same task for the entire network.

trices S^k map the amplitudes of the two incoming links onto the two outgoing ones. The unidirectional links represent the equipotential contours of the potential V and their random length is simulated by a random kinetic phase given to each link. The nodes represent the saddle points of V where the electrons can tunnel between contours. The tunneling amplitude T for each saddle point is given by $T = (1 + \exp((E - u_k)/E_t))^{-1/2}$,⁸⁾ where u_k is the energy of the saddle point with index k and E_t is the tunneling energy. E_t is of the form $E_t = \frac{l_c^2}{2\pi}c$, where c is the average curvature of the random potential which can be approximated by $c \approx V_0/l_V^2$ with $V_0 = \langle V^2 \rangle^{1/2}$. Taking into account that the saddle point energies are randomly distributed in the interval $[-W, W]$ gives us the following approximation for the tunneling energy:⁵⁾

$$E_t = W \left(\frac{l_c}{l_V} \right)^2. \quad (2)$$

This relation connects the quotient E_t/W which is the relevant parameter of the network model directly to the relevant parameter l_c/l_V of other smooth disorder models. It also connects the two limiting cases of the network model ($W/E_t = 0$ the original Chalker-Coddington case and $W/E_t = \infty$ the classical network percolation case) to the uncorrelated potential ($l_V=0$) and the classical motion in a magnetic field and random potential ($l_c = 0$) case.

The system shows an LD phase transition when E approaches the critical energy $E_c = \langle V \rangle = 0$. In this case the correlation length ξ scales as $\xi \propto |E - E_c|^\nu$, where $\nu \approx 2.3$. For large enough systems the correlation length exponent ν does not depend on W .⁴⁾ This is also true for other critical exponents like $\alpha_0 \approx 2.27$ determined by multifractal analysis of critical eigenfunctions.⁵⁾

A wave function or state of the network is defined by a normalized vector $\Psi = (\psi_1, \dots, \psi_n)$ whose elements ψ_i are the complex amplitudes on the $n = 2L^2$ network

links, where L is the system size. A wave function that at all nodes k of the network obeys the scattering condition $\psi_{l(i,k)} = \sum_j S_{ij}^k \psi_{l(j,k)}$, where $l(i,k)$ maps the matrix index $i \in \{0, 1, 2, 3\}$ of the scattering matrix S^k at node k to the respective link of the network, is stationary under scattering and therefore an eigenfunction of the system.

We can take all the matrix elements of the S^k and arrange them into a single operator U , so that the stationarity condition becomes

$$U(E)\Psi = \Psi. \quad (3)$$

The network operator U also functions as a time evolution operator for the network states, i.e. $\Psi(t + \tau) = U\Psi(t)$, where τ is the characteristic scattering time.^{9,10)} Equation (3) states that a wave function which is an eigenfunction of $U(E)$ with eigenvalue 1 is an eigenfunction of the modeled system. Such eigenfunctions will only occur at discrete values $E_n = E$ forming the eigenenergy spectrum of the system. These eigenenergies are not easily determined, but it was found in ref. 12 that the eigenvalues ω_α defined by the equation

$$U(E)\Psi_\alpha = e^{i\omega_\alpha(E)}\Psi_\alpha \quad (4)$$

for a fixed value of E show the same statistics as the eigenenergies E_n close to E . These so called quasienergies $\omega_\alpha(E)$ are much easier to determine. This and the fact that one can choose the exact point on the energy scale where we want to investigate the statistics make them the ideal tool for spectral investigations.^{12,13)} We can set $E = E_c$ and use all the critical quasienergies $\omega_\alpha(E_c)$, i.e. the eigenphases of $U(E_c)$ to determine spectral properties at criticality. This is an enormous advantage compared to other methods where only a small fraction of the spectrum is critical. We can even improve this method if we use the fact that for every eigenphase ω_α of the network operator the phase $\omega_\alpha + \pi$ (or in the case of double periodic boundary conditions the phases $\omega_\alpha + \pi/2$, $\omega_\alpha + \pi$ and $\omega_\alpha + 3\pi/2$) is also an eigenphase (see Appendix). This leads to a reduction of the matrix size increasing the speed of the numerical determination and also the attainable system sizes. Additionally, every eigenstate determined for a unitary operator $U(E_c)$ at the critical energy E_c is critical and can be used for multifractal analysis.^{5,9)}

§3. Percolation and Multifractality

Although percolation, i.e. $W > 0$, does not seem to have an influence on scaling and thereby on the result of the multifractal analysis, there are nevertheless some effects which have to be investigated.⁵⁾ They are very obvious if one looks at the wave functions themselves (see Fig. 2), but also show some influence in the scaling analysis.

The eigenstates in Fig. 2 obtained in the generalized network model at $E = E_c = 0$ show the typical self-similar shape of critical wave functions which led to the use of multifractal analysis on critical systems.¹⁵⁾ In this context the scale invariance of the eigenfunctions is

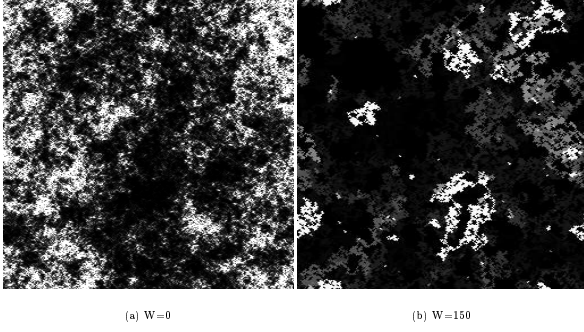


Fig. 2. Critical wave functions ($E = 0$) for $W = 0$ and $W = 150$. The system size is 256x256 saddle points. Darker areas denote lower square amplitude.

investigated by obtaining the following quantities:

$$m(l_b) = \int_{l_b^d} d\mathbf{r} |\Psi(\mathbf{r} + \mathbf{r}_0)|^2, \quad (5)$$

which denote the probability of a particle to be in a box of linear size l_b centered at \mathbf{r}_0 , respectively. The disorder averaged q -moments of $m(l_b)$, $m_q(l_b) = \langle m^q(l_b) \rangle$, scale over a wide range of box sizes with definite exponents,

$$m_q(\lambda) \propto \lambda^{d+\tau(q)}, \quad (6)$$

where $\lambda = l_b/L$ is the quotient of box size l_b to system size L . The exponents $\tau(q)$ depend non-linearly on q and characterize the universality class of the system. Often the single exponent $\alpha_0 = d\tau(q)/dq(q = 0)$ is used instead of the entire $\tau(q)$ spectrum, because it describes the scaling of the typical value of the squared amplitude with the system size, $\exp(\ln |\Psi|^2) \propto L^{-\alpha_0}$. The results of numerical investigations of these exponent show that they do not depend on the size of W (i.e. W/E_t , we will set $E_t = 1$ in the following).⁵⁾ However, we can observe that the range of box sizes for which scaling behavior is seen does change. For $W < 1$ the box probabilities scale over the entire range $a < l_b < L$, where a is the lattice constant of the network. If we increase W , scaling deteriorates for small box sizes, i.e. small λ 's. In Fig. 3 we show the $\ln[m^q(l_b)] - \ln \lambda$ -plots for four different values of W at $q = -0.5$. We see that the deterioration of scaling shows a significant dependence on W indicating that the valid range of lengths for scaling follows a law of the kind

$$a \left(\frac{W}{E_t} \right) < l_b < L, \quad (7)$$

where $a(x)$ is a function we have to determine.

If we take the values⁶⁾ of $\ln \lambda$ for each W at which the linear approximation becomes invalid and plot them against $\ln W$, a linear dependence becomes apparent (see Fig. 4). A linear fit of the data yields a slope of $X = 1.36 \pm 0.06$. Consequently, the minimal length where scaling can be seen follows the following relation

$$a \propto \left(\frac{W}{E_t} \right)^X. \quad (8)$$

Another effect of the increase of W are the increasing

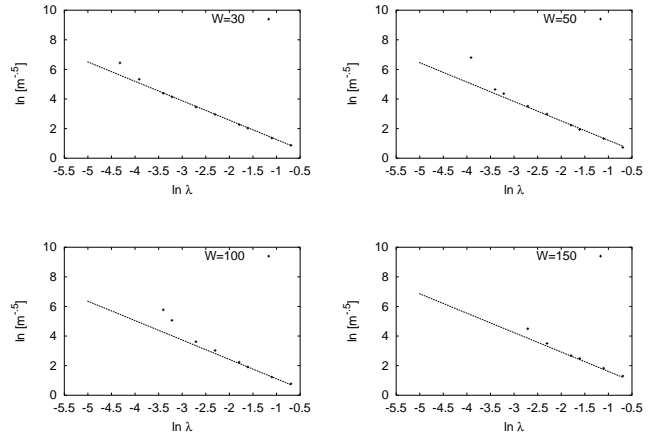


Fig. 3. The scaling of the average box-probabilities for different values of W at $q = -0.5$. System size $L = 250$.

sample to sample fluctuations and the rapid increase of the statistical error in the $f(\alpha)$ data, especially for large values of $|q|$. This all seems to be accompanied by a visible change of the characteristics of the wave function, as seen in Fig. 2. It is obvious that for $W = 150$ the wave function shows large areas, where the square amplitude changes only slightly, whereas for $W = 0$ such areas of constant amplitude are much smaller. In fact one can see a steady increase of the size of these areas if one gradually increases W .

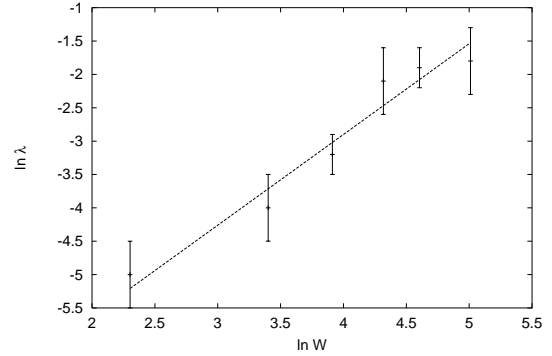


Fig. 4. The logarithms of the λ 's at which scaling deteriorates plotted against $\ln W$. As a result for the linear fit we get a slope of 1.36 ± 0.06

If we take all these effects into account, we have to conclude that, apparently, the introduction of variable saddle point energies, i.e. $W > 0$, leads to a new length scale in our system.

In order to understand how classical percolation can alter the shape of the quantum mechanical wave functions and influence their scaling behavior we will repeat the discussion published previously in literature.^{7,5,14)} Take a look at those saddle points whose energy u_k differs more than E_t from the electron energy $E = 0$. Of course, such saddle points occur only for $W > E_t$. The transmission coefficients T_k at these saddle points are exponentially small and the amplitude of an incoming link is essentially transmitted to a single outgoing link (classical behavior). Therefore, on a path avoiding sad-

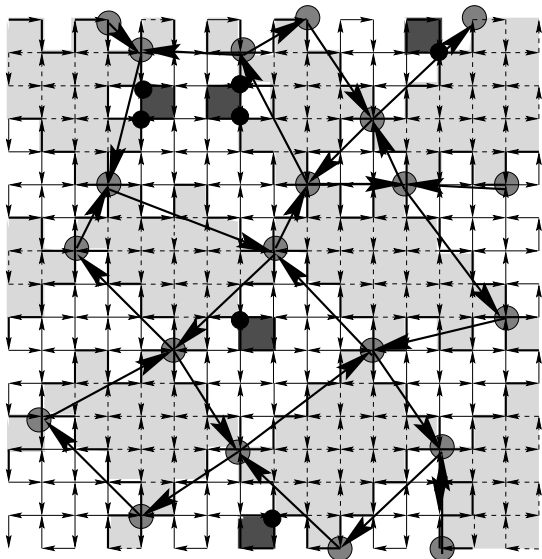


Fig. 5. Along the classical percolation path where the saddle point energies are large, $|u_k| > E_t$, the amplitude of the wave functions remain mainly constant. The resulting *critical* clusters form the links of the rescaled network.

dle points with energy $|u_k| < E_t$ the amplitude of the wave function remains mainly constant. This leads to the formation of clusters where the wave function amplitude changes only slightly (see Fig. 5). The size of these clusters is obviously connected to classical percolation. The cluster correlation length ξ_p of clusters connected by saddle points whose energy is smaller than E_t scales according to scaling theory (see e.g. refs. 16 and 17) as

$$\xi_p \propto \left(\frac{E_t}{W}\right)^{-\nu_p}. \quad (9)$$

This is the size of the largest clusters connected by those saddle points. If we consider that for smaller clusters, which connect via these saddle points to other large or small clusters, the effect in terms of the change of wave function amplitude along the percolation path will be negligible, we see that the relevant cluster size is of order ξ_p . Accordingly, not all saddle points with $u_k < E_t$ are relevant for the quantum mechanical effects, but only those *critical* saddle points that connect *critical* clusters and the scaling behavior of those clusters is given by (9). If we identify the clusters with the links of a new network and the saddle points with its nodes, we obtain a rescaled network model which has a renormalized lattice constant $a' = a(W/E_t)$ and a new $W' = E_t$. In this way, we can treat network models with arbitrarily large finite W by mapping it on the original Chalker–Coddington model.⁵⁾ Thus, we see that the influence of percolation is not on the overall scaling behavior but only on the range of the scaling. Its effects are mostly finite size effects which arise due to the decrease of the effective system size when we increase W .

One very strong finite size effect is the shift of the critical energy E_c when W is increased. This shift is not systematic but depends on the individual realization of the network. Due to the increasing range of the sad-

dle point energies when W increases the average value of saddle points energy for a single system is no longer $\langle u \rangle = 0$. Since the number of saddle points depends on the system size L , the number of random saddle point energies drawn from the square distribution may not be sufficient to guarantee that the deviation from the average is small when the W approaches the system size causing the critical point to shift to $E_c = -\langle u \rangle$ and consequently leading to strong fluctuations in the results for critical quantities. This suggests that any numerical investigations should be confined to values of W that obey $W < L$.

§4. Spectral Properties

The next step in our investigation is to see what happens to the spectral properties of the system when W is increased. In this case we are looking at the level spacing distribution $P(s)$ and at the level number variance $\Sigma_2(N) = \langle (n - \langle n \rangle)^2 \rangle$ of energy intervals containing on average $N = \langle n \rangle$ levels.

At the critical point $P(s)$ has a unique shape¹³⁾ which lies between the Poissonian behavior in the localized regime, $P(s) = \exp(-s)$, and that of the Gaussian unitary ensemble (GUE)-like in the metallic regime, $P(s) = \frac{32}{\pi^2} s^2 \exp(-\frac{4}{\pi} s^2)$, given by random matrix theory (RMT).²²⁾ For small s the level repulsion leads to a GUE-like behavior ($P(s) \propto s^2$), whereas for larger s the tail of the distribution behaves like $P(s) \propto \exp(-\kappa s)$, where $\kappa < 1$. This mixture between GUE and Poisson is due to the multifractal structure of the wave functions which are neither homogeneously smeared out over the entire system, as in the metallic regime, nor strongly localized. The direct connection between level distribution and multifractal wave function was found by Chalker et al.¹⁸⁾ when they derived for the compressibility $\chi = \lim_{N \rightarrow \infty} \lim_{L \rightarrow \infty} d\Sigma_2/dN$ at the critical point that $\chi = \frac{d-D_2}{2d}$, where d is the spatial and D_2 the fractal (correlation) dimension of the wave function. This equation could be verified numerically for the Chalker–Coddington network¹²⁾ and shows that we are again between the metallic ($\chi = 0$) and the localized ($\chi = 1$) behavior. If our arguments concerning the influence of classical percolation are valid, we should obtain the same kind of results for the critical spectra regardless of the value of W . On the other hand, we have seen that increasing W causes finite size effects to appear faster which should also be visible in the spectral properties.

We start by taking a look at the $P(s)$ distribution for different values of W . In Fig. 6 we can see $P(s)$ for $W = 0$ to $W = 40$. In this case we chose the system size $L = 80$, but we obtain the same $P(s)$ for other system sizes. The distribution is still system size independent at least for the range of system sizes we are able to investigate. This rules out finite size effects which could be expected due to the decrease of effective system size observed for the wave functions. Nevertheless, the distribution seems to become more and more Poissonian for larger W . This effect has already been seen by Ono et al.²¹⁾ who used the Landau model for the quantum Hall effect. In this case an increase of the potential's correlation length, which is

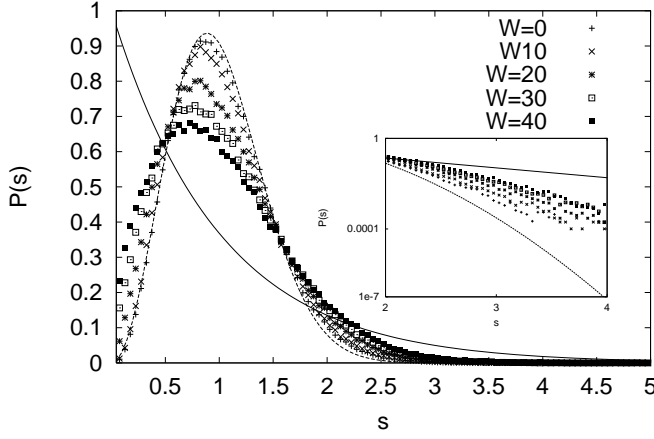


Fig. 6. The $P(s)$ spectrum for $W = 0, 10, 20, 30, 40$. The smooth curves show the Poisson and GUE distributions. The inset shows the same on a logarithmic scale.

according to eq. (2) comparable to an increase of W , led to a similar result. In their publication Ono et al. fitted the $P(s)$ distribution to the formula:

$$P(s) = As^\beta \exp(-Bs^\alpha), \quad (10)$$

where A and B are determined by the normalization conditions $\langle s \rangle = \langle 1 \rangle = 1$ and α and β are the fitting parameters. This way of fitting was prompted by the results of Kravtsov et al.,^{19,20} which predicted that $\beta = 2$ as for the Gaussian unitary ensemble (GUE), where $P(s) = \frac{32}{\pi^2} s^2 \exp(-4/\pi s^2)$, and $\alpha = 1 + 1/(d\nu) \approx 1.21$. Although, the numerical values for α do not fit that prediction^{21,13} we can still use eq. (10) to compare our data with that in ref. 21. The result of such a fit to the distributions in Fig. 6 is shown in Table I. We can see that $W \approx 30$

W	α		β	
0	1.54	± 0.02	2.03	± 0.03
10	1.71	± 0.04	1.96	± 0.05
20	1.79	± 0.02	1.30	± 0.02
30	1.94	± 0.03	0.85	± 0.01
40	2.04	± 0.03	0.59	± 0.01
l_c	1.52	$\pm 1.3 \times 10^{-4}$	1.95	$\pm 7.3 \times 10^{-4}$
$2l_c$	1.98	$\pm 5.7 \times 10^{-5}$	1.03	$\pm 1.6 \times 10^{-3}$

Table I. The results for the fit parameters α and β for different values of W . The last two entries give the values for different potential ranges determined by Ono et al.

corresponds to the results obtained by Ono et al. for a potential correlation length of $2l_c$, whereas a correlation length of l_c did not produce significant changes from the uncorrelated results (i.e. $W = 0$). We would expect that, because the relevant microscopic length in the Landau model is l_c so that the potential correlation length has to be larger to show an appreciable effect. This corresponds to the fact that $W \approx E_t$ also has no effect since the tunnel energy E_t sets the energy scale for our system and W has to be larger in order to obtain *classical* saddle

points.

For both models it is very clear that the level repulsion for small values of s decreases with increasing W and correlation length, respectively. This is indicated by the increase of $P(s = 0)$ and the decrease of the fit parameter β .

In ref. 13 it was found that the tail of $P(s)$ shows an exponential decay of the form $P(s) \propto \exp(-\kappa s)$, which was predicted by Altshuler et al.²³ with $\kappa = 1/(2\chi)$ and confirmed for QHE systems by the numerical results in refs. 13 and 24. In Fig. 7 we show the behavior of the tail region of $P(s)$ for different W . Although the tail seems to remain an exponential the factor κ decreases with increasing W getting closer to the Poissonian behavior, where $\kappa = 1$. This would indicate that the com-

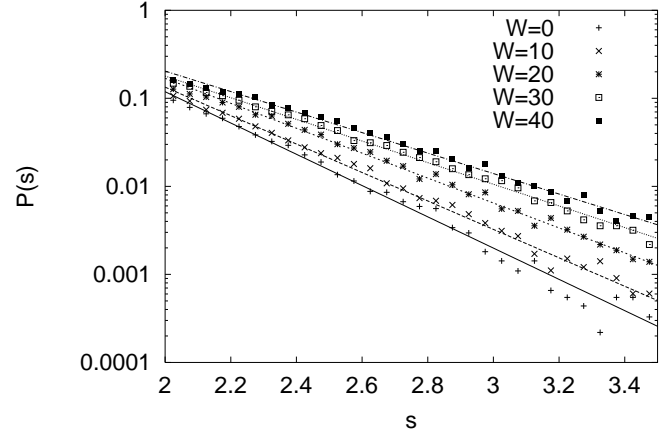


Fig. 7. The tail of the $P(s)$ spectrum for $W = 0, 10, 20, 30, 40$. The smooth curves are the linear fits for respective curves.

pressibility χ also changes with W . In Fig. 8 we show the level number variance $\Sigma_2(N)$ from which we obtain χ by determining its slope. We can see that the slope increases with increasing W which would correspond to the decrease of κ , but a look at Table II shows that the relation $\kappa = 1/(2\chi)$ no longer holds in the case $W > 0$.

W	κ		χ		$1/(2\chi)$	
0	4.09	± 0.10	0.127	± 0.002	3.94	± 0.06
10	3.72	± 0.06	0.190	± 0.003	2.63	± 0.04
20	3.26	± 0.05	0.254	± 0.001	1.96	± 0.01
30	2.83	± 0.04	0.291	± 0.002	1.71	± 0.01
40	2.68	± 0.04	0.313	± 0.002	1.59	± 0.01

Table II. The results for κ and χ for different values of W .

This is also true for the relation $\chi = \frac{d-D_2}{2d}$ connecting the compressibility χ to the multifractal exponent D_2 .²⁵ From the investigation of the critical wave functions we know that D_2 does not change with W .

Finally, observing that increasing W has a strong effect on the shape of $P(s)$ the question arises whether a function like

$$J_0(L, E) = \frac{1}{2} \langle s^2 \rangle_{L, E}, \quad (11)$$

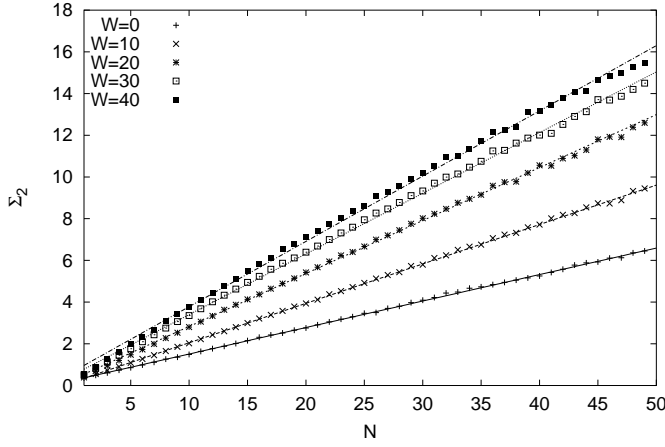


Fig. 8. The function $\Sigma(N)$ for different values of W .

which depends on as well as describes the shape of $P(s)$ still shows the same one-parameter scaling for $W > 0$ as for $W = 0$. The insets in Fig. 9 shows J_0 for $W = 5, 15$ as a function of E for different system sizes. At the critical point $E_c = 0$ all curves come together at a single size independent point which varies with W reflecting the dependence of the shape of $P(s)$ on W . If one-parameter scaling still holds then a scaling function f of the following form should exist:

$$J_0(E, L) = f(L/\xi), \quad \xi = \xi_0 |E - E_c|^{-\nu}. \quad (12)$$

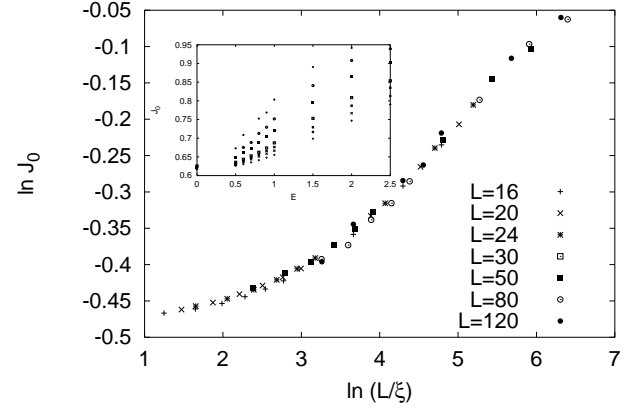
We determined $f(x)$ by fitting a fourth degree polynomial in $x = \ln(L/\xi_0) + \nu \ln E$ to our data using ξ_0 and ν as fitting parameters. The values we found for ν and the critical values of J_0 are given in Table III. Although the critical values $J_0^c(W)$ vary systematically with W the scaling exponent ν shows no systematic dependence on W and is consistent with previous results for ν obtained by various studies^{26, 27, 28, 29, 30} within the error bars.

W	ν		J_0^c	
0	2.1	± 0.3	0.600	± 0.005
2	2.1	± 0.2	0.601	± 0.01
5	2.2	± 0.1	0.604	± 0.01
10	2.1	± 0.3	0.611	± 0.01
15	2.3	± 0.1	0.623	± 0.01
30	2.3	± 0.4	0.664	± 0.01
40	2.2	± 0.3	0.685	± 0.01

Table III. The results for the scaling exponent ν and the critical value of J_0 for different values of W .

§5. Conclusion

In this paper we have discussed the influence of percolation effects on critical wave functions and the critical quasienergy spectrum of the Chalker–Coddington network model. Classical percolation effects appear in the generalized version of the model when the range W of the saddle point energies, i.e. node energies of the network, is increased from $W = 0$ in the original model to



(a) $W=5$

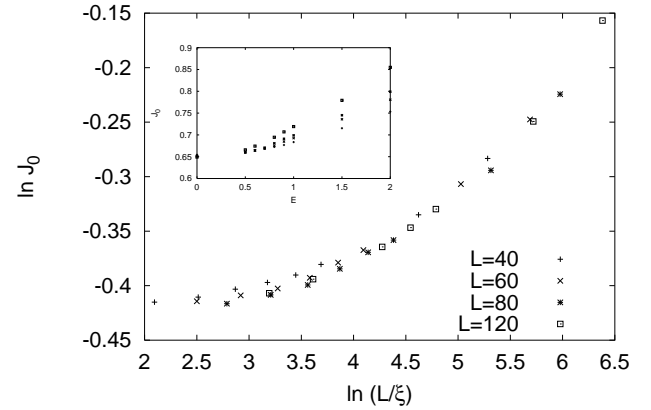


Fig. 9. The one-branch scaling functions $J_0(L/\xi)$ for four different values of W resulting from the rescaling of the function $J_0(E, L)$ shown in the insets.

$W > 1$.

We found that multifractal analysis of the critical wave functions results in the same exponents regardless of the value of W . Nevertheless, we can see the effect of classical percolation in the appearance of a new microscopic length scale which increases with W and scales with an exponent $X = 1.36 \pm 0.06$ consistent with the exponent $\nu_p = 4/3$ of the classical correlation length. This confirms the connection of the correlation length to that new length scale, which sets the minimum length for scaling and therefore reduces the effective size of the system, thereby causing increasing fluctuations when W grows.

In the case of the spectral statistics of the quasienergies of the network the influence of an increasing W is more profound. An increasing shift from the critical statistics towards Poissonian behavior is observed for all the spectral quantities we have investigated. Although this shift does not seem to have an influence on the scaling exponent ν it is clearly visible. Since the effect is not changing with system size, it can not be ruled as a mere finite size effect resulting from the decrease of effective system size observed for the critical wave functions. Furthermore, we observed that the changes that come with an increase of W are very similar to those connected with

the increase of the potential correlation length observed by Ono et al.²¹⁾

It seems, although the multifractal behavior of the critical wave functions is well understood, that more elaborate analytical studies are indicated to understand the level statistics at the LD transition.

Acknowledgments

The author would like to thank Y. Ono and I. Varga for useful discussions. This work was supported by the Deutsche Forschungsgemeinschaft (DFG) postdoc program.

Appendix: Degeneracy of Eigenvalues

The chiral structure of the Chalker-Coddington network leads to a pseudo degeneracy of the eigenvalues of its network operator U . For each eigenvector Ψ_α with eigenvalue $e^{i\omega_\alpha}$ there exists an eigenvector $\tilde{\Psi}_\alpha$ with eigenvalue $e^{i(\omega_\alpha+\pi)}$.

In order to prove this, let us first point out the fact that the operator U maps vertical links only to horizontal links and vice versa. This means that U^2 maps vertical to vertical and horizontal to horizontal links, thereby creating two orthogonal U^2 -invariant subspaces. We can therefore define the projection operators P_v and P_h which will project onto the two subspaces, respectively.

Let Ψ_α be an eigenvector of U with eigenvalue $e^{i\omega_\alpha}$. Then Ψ_α is also an eigenvector of U^2 with eigenvalue $e^{2i\omega_\alpha}$. We can write Ψ_α as a linear combination of the two projections $\Psi_\alpha^v = P_v \Psi_\alpha$ and $\Psi_\alpha^h = P_h \Psi_\alpha$:

$$\Psi_\alpha = \Psi_\alpha^v + \Psi_\alpha^h = v\mathbf{e}_\alpha^v + h\mathbf{e}_\alpha^h, \quad (\text{A.1})$$

where $v = |\Psi_\alpha^v|$, $h = |\Psi_\alpha^h|$, $\mathbf{e}_\alpha^v = v^{-1}\Psi_\alpha^v$ and $\mathbf{e}_\alpha^h = h^{-1}\Psi_\alpha^h$. Since Ψ_α^v and Ψ_α^h are orthogonal to each other they are both also eigenvectors of U^2 with eigenvalue $e^{2i\omega_\alpha}$. This means that this eigenvalue is degenerate.

Let us now construct the following eigenvector of U^2 :

$$\tilde{\Psi}_\alpha = h\mathbf{e}_\alpha^v - v\mathbf{e}_\alpha^h.$$

$\tilde{\Psi}_\alpha$ is obviously orthogonal to Ψ_α . In order to see what will happen if we use U on $\tilde{\Psi}_\alpha$, let us first use it on Ψ_α and keep in mind that $U\mathbf{e}_\alpha^h = e^{i\omega_h}\mathbf{e}_\alpha^v$ and $U\mathbf{e}_\alpha^v = e^{i\omega_v}\mathbf{e}_\alpha^h$, where $e^{2i\omega_v} = e^{2i\omega_h} = e^{2i\omega_\alpha}$.

$$U\Psi_\alpha = v e^{i\omega_v}\mathbf{e}_\alpha^h + h e^{i\omega_h}\mathbf{e}_\alpha^v = e^{i\omega_\alpha}\Psi_\alpha. \quad (\text{A.2})$$

From eqs. (A.2) and (A.1) it follows that $v = h e^{i(\omega_\alpha - \omega_v)}$ and $h = v e^{i(\omega_\alpha - \omega_h)}$ and consequently

$$\begin{aligned} U\tilde{\Psi}_\alpha &= h e^{i\omega_v}\mathbf{e}_\alpha^h - v e^{i\omega_h}\mathbf{e}_\alpha^v \\ &= e^{2i(\omega_\alpha - \omega_v)} h e^{i\omega_v}\mathbf{e}_\alpha^h - e^{2i(\omega_\alpha - \omega_h)} v e^{i\omega_h}\mathbf{e}_\alpha^v \\ &= e^{i\omega_\alpha} \left[h e^{i(\omega_\alpha - \omega_v)}\mathbf{e}_\alpha^h - v e^{i(\omega_\alpha - \omega_h)}\mathbf{e}_\alpha^v \right] \\ &= -e^{i\omega_\alpha} [-v\mathbf{e}_\alpha^h + h\mathbf{e}_\alpha^v] \\ &= -e^{i\omega_\alpha}\tilde{\Psi}_\alpha. \end{aligned}$$

This means $\tilde{\Psi}_\alpha$ is an eigenvector of U with eigenvalue $e^{i(\omega_\alpha+\pi)}$.

The same kind of argument leads to a further pseudo-degeneracy when we impose double periodic boundary conditions (torus) with system size L a multiple of 2. In that case each eigenphase ω_α is accompanied by three other eigenphases $\omega_\alpha + \pi/2$, $\omega_\alpha + \pi$ and $\omega_\alpha + 3\pi/2$. This is caused by the chiral symmetry above and the boundary conditions which lead to the formation of two more (in this case U^4) invariant subspaces within each of the U^2 -invariant subspaces of vertical and horizontal lines. These subspaces consist of the sets combining every second vertical row or every second horizontal column, respectively. Without the boundary conditions those subspaces mix.

-
- [1] J. T. Chalker, P. D. Coddington, J. Phys. C **21**, 2665 (1988).
 - [2] M. Janssen, O. Viehweger, U. Fastenrath and J. Hajdu: *Introduction to the Theory of the Integer Quantum Hall Effect* (VCH, Weinheim; New York; Basel; Cambridge; Tokyo, 1994).
 - [3] J. F. G. Eastmond, Ph. D. thesis, Oxford University (1992).
 - [4] D. H. Lee, Z. Wang and S. Kivelson: Phys. Rev. Lett. **70**(1993) 4130.
 - [5] R. Klesse and M. Metzler, Europhys. Lett. **32**(1995) 229.
 - [6] We read the data directly from plots like in Fig. 3 with error bars corresponding to the possible errors made by doing so.
 - [7] D. G. Polyakov and M. E. Raikh: Phys. Rev. Lett. **75**(1995) 1368.
 - [8] H. A. Fertig: Phys. Rev. B **38**(1988) 996.
 - [9] R. Klesse and M. Metzler, to be published.
 - [10] R. Klesse, Ph.D. Thesis, Universität zu Köln, (AWOS-Verlag, Erfurt) 1996.
 - [11] B. Huckestein and R. Klesse: Phys. Rev. B **55**(1997) R7303.
 - [12] R. Klesse and M. Metzler: Phys. Rev. Lett. **79**(1997) 721.
 - [13] M. Metzler and I. Varga, J. Phys. Soc. Jpn. **67**, 1856 (1998).
 - [14] M. Metzler, Ph.D. Thesis, Universität zu Köln 1996.
 - [15] M. Janssen: Int. J. Mod. Phys. **8**(1994) 943.
 - [16] M.B. Isichenko, Rev. Mod. Phys. **64**, 961 (1992).
 - [17] D. Stauffer: *Introduction to Percolation Theory*, Taylor & Francis, 1985.
 - [18] J. T. Chalker, V. E. Kravtsov and I. V. Lerner: JETP Lett. **64**(1996) 386.
 - [19] V. E. Kravtsov, I. V. Lerner, B. L. Altshuler and A. G. Aronov: Phys. Rev. Lett. **72**(1994) 888.
 - [20] A. G. Aronov, V. E. Kravtsov and I. V. Lerner: JETP Lett. **59**(1994) 39.
 - [21] Y. Ono, T. Ohtsuki and B. Kramer: J. Phys. Soc. Jpn. **65**(1996) 1734.
 - [22] M. L. Mehta: *Random Matrices*, 2nd ed. (Academic Press, New York, 1991).
 - [23] B. L. Altshuler, I. Kh. Zharekeshev, S. A. Kotochigova and B. Shklovskii: Sov. Phys.-JETP **67**(1988) 625.
 - [24] M. Batsch and L. Schweitzer: *High Magnetic Fields in the Physics of Semiconductors II: Proceedings of the International Conference, Würzburg 1996*, edited by G. Landwehr and W. Ossau (World Scientific Publishers Co., Singapore, 1997), pp. 47–50.
 - [25] Both relations do not hold for the localized regime where $\chi = 1 \neq 1/2$. This is to be expected since the assumptions made for their derivation are not valid in the localized regime. (See also ref. 18).
 - [26] H. Aoki and T. Ando: Phys. Rev. Lett. **54**(1985) 831.
 - [27] B. Huckestein and B. Kramer: Phys. Rev. Lett. **64**(1990) 1473.
 - [28] Y. Huo and R. N. Bhatt: Phys. Rev. Lett. **68**(1992) 1375.
 - [29] Dongzi Liu and S. Das Sarma: Phys. Rev. B **49**(1994) 2677.
 - [30] T. Ohtsuki and Y. Ono: J. Phys. Soc. Jpn. **64**(1995) 4088.